# A Theoretical Basis for Low Barriers in Transition-Metal Complex $2_\pi + 2_\pi$ Reactions: The Isomerization of $Cp_2TiC_3H_6$ to $Cp_2TiCH_2(C_2H_4)$

**T. H. Upton*[†] and A. K. Rappé*[‡]**

*Contribution from the Corporate Research—Science Laboratories, Exxon Research and Engineering, Annandale, New Jersey 08801, and the Department of Chemistry, Colorado State University, Fort Collins, Colorado 80523.* *Received March 12, 1984*

**Abstract:** The interconversions of transition-metal alkylidene–olefin complexes with corresponding metallacycles are formally $2_\pi + 2_\pi$ processes. Conventionally, such reactions would be expected to possess large activation barriers, yet for these transition-metal systems this is often not true. One such reaction is the isomerization of the stable complex dicyclopentadienyltitanacyclobutane to an ethylene–titanium methylidene complex. We have explored the evolution of the electronic structure in the analogous rearrangement of dichlorotitanacyclobutane to its corresponding olefin–titanium methylidene complex, characterizing in detail the wave functions and energetics of each complex and the transition state connecting them. We find no activation barrier for the rearrangement, and the metallacycle is more stable than the olefin–alkylidene complex by 12 kcal/mol. We demonstrate that the state evolution in this reaction is governed by the same Pauli principle constraints that often lead to high barriers in other reactions of this type. We show that the participation of a 3d orbital allows satisfaction of these constraints in a unique way that avoids the unfavorable transition-state bonding interactions that are usually the source of a high barrier.

## I. Introduction

Olefin[1] and acetylene metathesis,[2] olefin oxidation,[3] and olefin polymerization[4] reactions are transition-metal-assisted reactions that occur quite easily with early transition metals. They generally have low energies of activation, and all have (or are likely to have) "forbidden" key steps (assuming the metal–ligand bonds are at least moderately covalent). For example, the Arrhenius activation energy for olefin metathesis has been measured[1a] to be as low as 6.6 kcal/mol. The chromyl chloride oxidation of aliphatic alkenes[3a] has an enthalpy of activation of around 6.0 kcal/mol. The corresponding oxidations of substituted styrenes have activation enthalpies[3b] ranging from 2.0 to 9.0 kcal/mol. The activation energies for olefin polymerization range from 6.0[4a] to 12.0[4b] kcal/mol.

Each of these processes has been suggested to involve the addition of a carbon–carbon $\pi$ bond across a metal–ligand $\pi$ bond. If such bonds are considered to be at least partially covalent, then each of these processes is a thermal 2 + 2 reaction, predicted to be "forbidden" by a variety of rules. Specifically, the Woodward–Hoffmann rules,[5] Fukui's frontier orbital approach,[6] Pearson's perturbational overlap approach,[7] and valence-bond approaches by van der Hart, Mulder, and Oosterhoff[8] and by Epiotis[9] all suggest that these reactions should not occur thermally.

Upton[10] has recently demonstrated that an alternate analysis based upon the Pauli principle rather than orbital symmetry explains the low barriers observed for metal surface catalytic processes and the types of processes described above. The approach is an extention of concepts outlined in the orbital phase continuity principle put forth by Goddard.[11] As presented by Upton it provides a rational explanation for the importance of d orbitals in transition-metal-surface-catalyzed reactions.

In this study we show that these concepts are directly applicable to the class of 2 + 2 additions involving transition-metal centers outlined above. Specifically, we consider the isomerization of the parent dichlorotitanacyclobutane to form an ethylene–titanium methylidene complex.

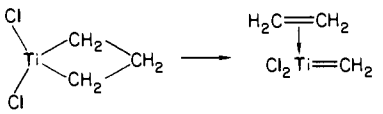


(1)

[†] Exxon Research and Engineering.
[‡] Colorado State University.

Previous work[12] has shown this chloride system to be a reasonable structural and energetic model of dicyclopentadienyl-

(1) (a) Hughes, W. B. *J. Am. Chem. Soc.* **1970**, *92*, 532-537. (b) Grubbs, R. H. *Prog. Inorg. Chem.* **1978**, *24*, 1-50. (c) Calderon, N.; Lawrence, J. P.; Ofstead, E. A. *Adv. Organomet. Chem.* **1979**, *17*, 449-492.

(2) (a) Pannella, F.; Banks, R. L.; Bailey, g. C. *J. Chem. Soc., Chem. Commun.* **1968**, 1548-1549. (b) Moulijn, J. A.; Reitsma, H. J.; Boelhouwer, C. *J. Catal.* **1972**, *25*, 434-436. (c) Mortreux, A.; Delgrange, J. C.; Blanchard, M.; Labochinsky, B. *J. Mol. Catal.* **1977**, *2*, 73. (d) Devarajan, S.; Walton, O. R. M.; Leigh G. J. *J. Organomet. Chem.* **1979**, *181*, 99-104. (e) Katz, T. J. *J. Am. Chem. Soc.* **1975**, *97*, 1592-1594. (f) Clark, D. N.; Schrock, R. R. *Ibid.* **1978**, *100*, 6774-6776. (g) Wengrovius, J. H.; Sancho, J.; Schrock, R. R. *Ibid.* **1981**, *103*, 3932-3934. (h) Schrock, R. R.; Listemann, M. L.; Sturgeoff, L. G. *Ibid.* **1982**, *104*, 4291-4293. (i) Pedersen, S. F.; Schrock, R. R.; Churchill, M. R.; Wasserman, H. J. *Ibid.* **1982**, *104*, 6808-6809. (j) Bencheikh, A.; Petit, M.; Mortreux, A.; Petit, F. *J. Mol. Catal.* **1982**, *15*, 93-101. (k) Petit, M.; Mortreux, A.; Petit, F. *J. Chem. Soc., Chem. Commun.* **1982**, 1385-1386.

(3) (a) Freeman, F.; McMart, P. D.; Yamachika, N. J. *J. Am. Chem. Soc.* **1970**, *92*, 4621-4626. (b) Freeman, F.; Yamachika, N. J. *Ibid.* **1972**, *94*, 1214-1219. (c) Hartford, W. H.; Darrin, M. *Chem. Rev.* **1958**, *58*, 1-61. (d) Wiberg, K. B. "Oxidation in Organic Chemistry"; Academic Press: New York, 1965; Part A, pp 69-184. (e) Freeman, F. *Rev. React. Species Chem. React.* **1973**, *1*, 37-64.

(4) (a) Fink, G.; Rottler, R.; Schnell, D.; Zoller, W. *J. Appl. Polymer Sci.* **1976**, *20*, 2779-2790. (b) Chien, J. C. W. *J. Am. Chem. Soc.* **1959**, *81* 86-92. (c) Sinn, H.; Kaminsky, W. *Adv. Organomet. Chem.* **1980**, *18*, 99-149. (d) Pino, P.; Mulhaupt, R. *Angew. Chem., Int. Ed. Engl.* **1980**, *19*, 857-875. (e) Ivin, K. J.; Rooney, J. J.; Stewart, C. D.; Green, M. L. H.; Mahtab, R. *J. Chem. Soc., Chem. Commun.* **1978**, 604-606. (f) Watson, P. L. *J. Am. Chem. Soc.* **1982**, *104*, 337-339. (g) Turner, H. W.; Schrock, R. R. *Ibid.* **1982**, *104*, 2331-2333. (h) Soto, J.; Steigerwald, M. L.; Grubbs, R. H. *Ibid.* **1982**, *104*, 4479-4480. (i) Brookhart, M.; Green, M. L. H. *J. Organomet. Chem.* **1983**, *250*, 395-408. (j) Turner, H. W.; Schrock, R. R.; Fellmann, J. D.; Holmes, S. J. *J. Am. Chem. Soc.* **1983**, *105*, 4942-4950.

(5) Woodward, R. B.; Hoffmann, R. *J. Am. Chem. Soc.* **1965**, *87*, 395-397. Woodward, R. B.; Hoffmann, R. "The Conservation of Orbital Symmetry"; Verlag Chemie: Weinheim/Berstr., Germany, 1970.

(6) Fukui, H. *Bull. Chem. Soc. Jpn.* **1966**, *39*, 498-503. Fukui, H. *Acc. Chem. Res.* **1971**, *4*, 57-64.

(7) Pearson, R. G. "Symmetry Rules for Chemical Reactions"; Wiley-Interscience: New York, 1976.

(8) van der Hart, W. J.; Mulder, J. J. C.; Oosterhoff, L. J. *J. Am. Chem. Soc.* **1972**, *94*, 5724-5730.

(9) Epiotis, N. D. "United Valence Bond Theory of Electronic Structure"; Springer-Verlag: New York, 1982.

(10) Upton, T. H. *J. Am. Chem. Soc.* **1984**, *106*, 1561.

0002-7863/85/1507-1206$01.50/0 

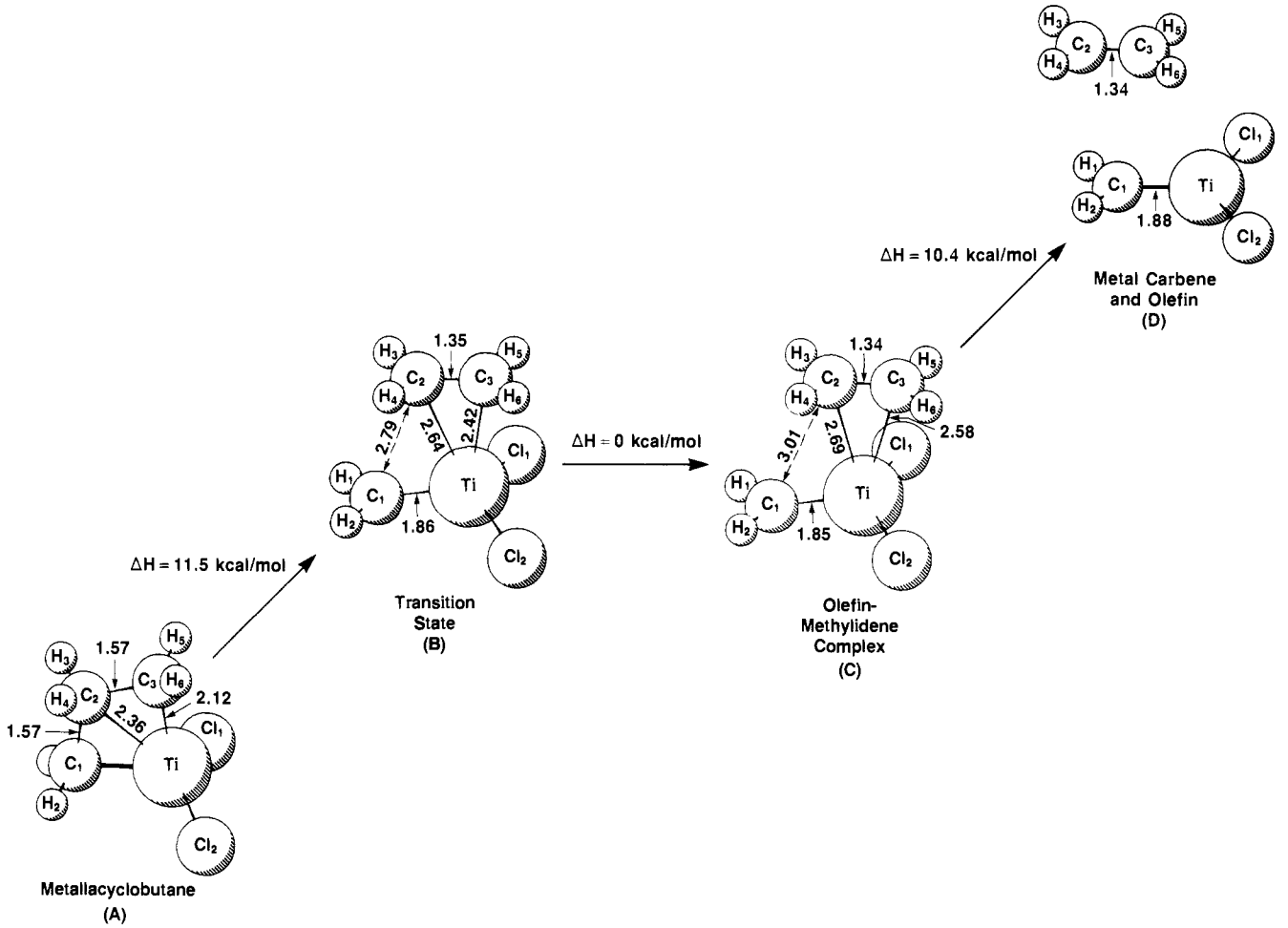


**Figure 1.** Calculated geometries and enthalpy changes (298 K) for (A) the parent titanacyclobutane, (B) the reaction transition state, (C) the product ethylene–titanium methylidene complex, and (D) isolated titanium–methylidene and ethylene moieties. Bond distances are in angstroms.

titanacyclobutane, a moderately active olefin metathesis catalyst.[13] We present calculations characterizing the initial metallacycle and the final olefin–methylidene complex as well as the transition state connecting them. We find the transition state to be essentially degenerate with the product state. By following an approximation to the reaction coordinate, we show that the low barrier and state evolution that occur are in keeping with Pauli principle requirements that are unique to transition-metal-based reactions.

Details of the reaction pathway and a discussion of the chemistry obtained from the calculations are given in the next section. Following this, we review those theoretical concepts needed to understand the state evolution and energetic character of the reaction path. Finally we extend our results to the above-mentioned systems.

**Table I.** Summary of Geometric Parameters for the Metallacyclobutane Complex

| center | *x* | *y* | *z* |
|---|---|---|---|
| | (a) Atomic Coordinates (au) | | |
| Ti | 0.00 | 0.00 | 0.00 |
| Cl1 | 1.217 183 98 | −1.217 183 97 | −4.009 077 26 |
| Cl2 | 1.217 183 98 | −1.217 183 97 | 4.009 077 26 |
| C1 | −3.970 059 46 | 0.537 055 33 | 0.00 |
| C2 | −3.471 284 32 | 3.471 284 31 | 0.00 |
| C3 | −0.537 055 33 | 3.970 059 45 | 0.00 |
| H1 | −4.774 029 20 | −0.266 914 41 | −1.694 770 93 |
| H2 | −4.774 029 20 | −0.266 914 41 | 1.694 770 93 |
| H3 | −4.292 621 40 | 4.292 621 39 | −1.671 432 47 |
| H4 | −4.292 621 40 | 4.292 621 39 | 1.671 432 47 |
| H5 | 0.266 914 41 | 4.774 029 19 | −1.694 770 93 |
| H6 | 0.266 914 41 | 4.774 029 19 | 1.694 770 93 |

| | | | |
|---|---|---|---|
| (b) Selected Bond Lengths (Å) and Angles (deg) | | | |
| $Ti-Cl_1,Cl_2$ | 2.31 | $C_1-C_3$ | 2.57 |
| $Ti-C_1$ | 2.12 | $C_2-C_3$ | 1.57 |
| $Ti-C_2$ | 2.60 | $C_1-H_1,H_2$ | 1.08 |
| $Ti-C_3$ | 2.12 | $C_2-H_3,H_4$ | 1.08 |
| $C_1-C_2$ | 1.57 | $C_3-H_5,H_6$ | 1.08 |
| $Ti-C_1-C_2$ | 88.1 | $H_3-C_2-H_4$ | 110.4 |
| $Ti-C_2-C_1$ | 54.6 | $H_5-C_3-H_6$ | 112.3 |
| $Ti-C_3-C_2$ | 88.1 | $Ti-C_1-H_1,H_2$ | 109.7 |
| $Ti-C_2-C_3$ | 54.6 | $C_2-C_3-H_5,H_6$ | 117.0 |
| $C_1-Ti-C_3$ | 74.6 | $C_3-C_2-H_3,H_4$ | 109.3 |
| $C_1-Ti-C_2$ | 37.3 | $Cl_1-Ti-Cl_2$ | 133.5 |
| $C_2-Ti-C_3$ | 37.3 | $Cl_1,Cl_2-Ti-C_1$ | 108.3 |
| $C_1-C_2-C_3$ | 109.2 | $Cl_1,Cl_2-Ti-C_2$ | 113.2 |
| $H_1-C_1-H_2$ | 112.3 | $Cl_1,Cl_2-Ti-C_3$ | 108.3 |

(11) (a) Wilson, C. W., Jr.; Goddard, W. A., III *J. Chem. Phys.* **1969**, *51*, 716–731. (b) Goddard, W. A., III; Ladner, R. C. *Int. J. Quantum Chem., Symp.* **1969**, *3*, 63–66. (c) Goddard, W. A., III; *J. Am. Chem. Soc.* **1970**, *92*, 7520–7521. (d) Goddard, W. A., III; Ladner, R. C. *Ibid.* **1971**, *93*, 6750–6756. (e) Goddard, W. A., III. *Ibid.* **1972**, *94*, 793–807. (f) Wilson, C. W., Jr.; Goddard, W. A., III *J. Chem. Phys.* **1972**, *56*, 5913–5920. (g) Levin, G.; Goddard, W. A., III *J. Am. Chem. Soc.* **1975**, *97*, 1649–1656. (h) Walch, S. P.; Dunning, T. H., Jr. *J. Chem. Phys.* **1980**, *72*, 1303–1311. (i) Dunning, T. H., Jr. *Ibid.* **1980**, *73*, 2304–2309. (j) Dunning, T. H., Jr.; Walch, S. P.; Goodgame, M. M. *Ibid.* **1981**, *74*, 3482–3488. (k) Harding, L. B. *J. Phys. Chem.* **1981**, *85*, 10–11. (i) Harding, L. B. *J. Am. Chem. Soc.* **1981**, *103*, 7469–7475. (m) Subsequent to the completion of this work a study of the similar $2_\sigma + 2_\sigma$ reaction for transition-metal complexes appeared: Steigerwald, M. L.; Goddard, W. A., III *Ibid.* **1984**, *106*, 308–311.

(12) (a) Rappé, A. K.; Goddard, W. A., III *J. Am. Chem. Soc.* **1982**, *104*, 297–299. (b) Francl, M. M.; Pietro, W. J.; Hout, R. F.; Hehre, W. J. *Organometallics* **1983**, *2*, 281–286.

(13) (a) Howard, T. R.; Lee, J. B.; Grubbs, R. H. *J. Am. Chem. Soc.* **1980**, *u02*, 6876–6878. (b) Lee, J. B.; Gajda, G. J.; Schaefer, W. P.; Howard, T. R.; Ikariya, T.; Straus, D. A.; Grubbs, R. H. *Ibid.* **1981**, *u03*, 7358–7361. (c) Lee, J. B.; Ott, K. C.; Grubbs, R. H. *Ibid.* **1982**, *104*, 7491–7496. (d) Straus, D. A.; Grubbs, R. H. *Organometallics* **1982**, *1*, 1658–1661.

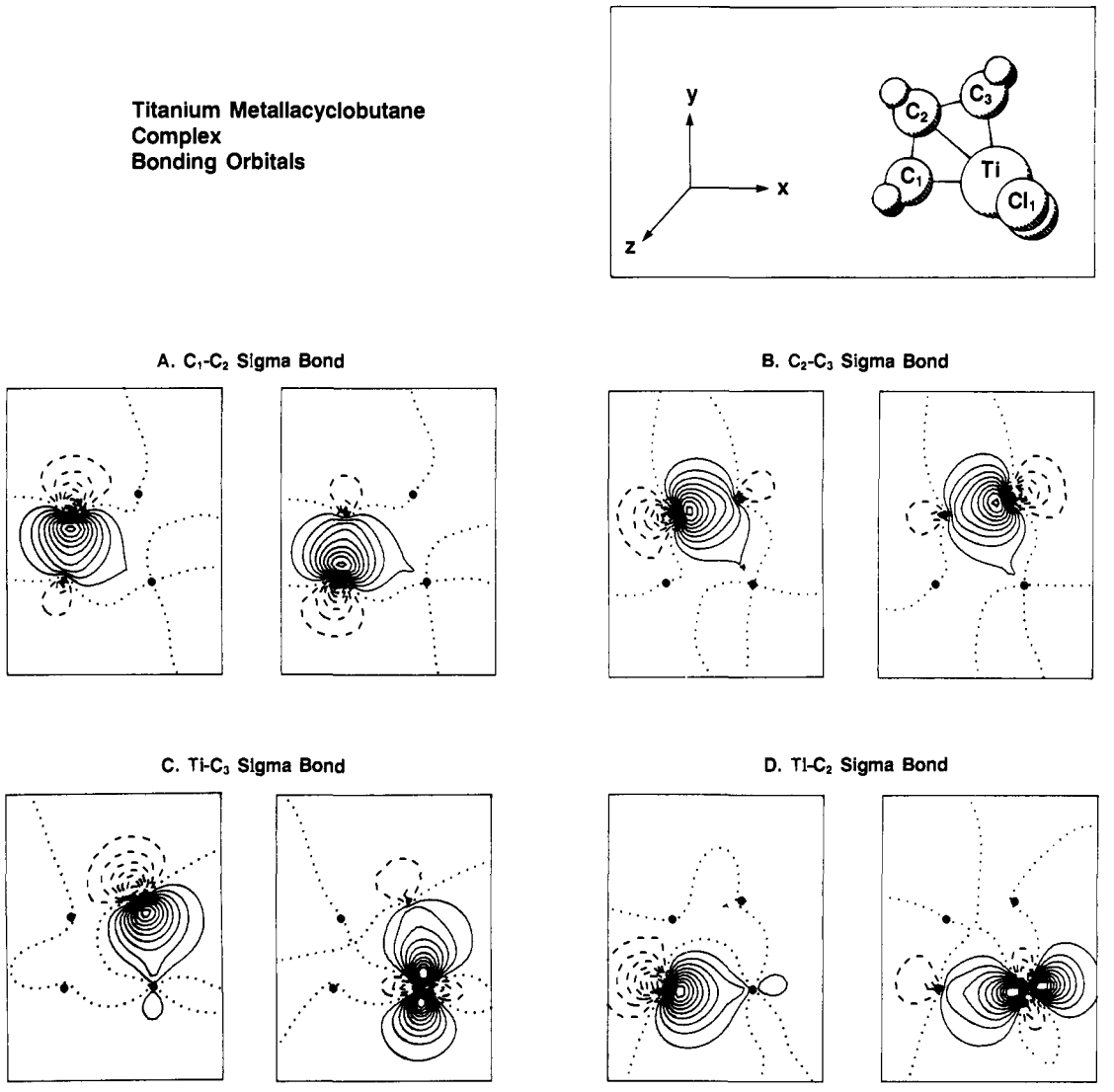


**Figure 2.** Contour plots of GVB orbitals defining the metallacycle $\sigma$ bonds in the parent dichlorotitanacyclobutane complex. The molecular geometry is shown at upper right. The orbital plotting plane contains the four atoms forming the ring skeleton. They are located in each orbital plot at approximately the relative positions shown at upper right and marked with a filled circle. The solid contours define positive orbital amplitude, and the dotted lines are nodal lines.

## II. Overview of the Metallacycle Reaction

We begin with a brief structural characterization of the parent metallacycle, the product olefin–methylidene complex, and the reaction transition state as they appear in the calculations. Following this, we will examine the molecular transformation that occurs along the reaction coordinate in detail. Our results are compared with available experimental data, as well as the results of theoretical studies that have been carried out on this and related systems.

**A. The Dichlorotitanacyclobutane Complex.** The geometry of the metallacycle is shown schematically in Figure 1A, and geometric parameters of the complex are summarized in Table I. The ring skeleton was constrained to be planar during the calculations, and the final geometry displays $C_{2v}$ symmetry. Carbon–carbon bond distances (1.57 Å) are comparable to typical aliphatic carbon–carbon distances. The configuration at $C_2$ is nearly tetrahedral, indicating an absence of both unsaturated character and ring strain at that position. There are substantial departures from tetrahedral configurations at $C_1$ and $C_3$, with extremely small skeletal angles of 88.1°. The cyclopentadienyl analogue of this metallacycle, dicyclopentadienyltitanacyclobutane, displays a similar arrangement of bond lengths and angles at the carbon atoms.[13b] Our calculated Ti–C bond lengths of 2.12 Å are also in good agreement with the observed 2.15 Å.

To aid in further examining the character of the bonding about the titanium atom, we provide contour plots of the metallacycle bonding orbitals in Figure 2. The orbitals shown here are generalized valence bond (GVB) orbitals,[14] obtained by allowing each electron of a bonding electron pair to have its own orbital (see Appendix). When the orbitals of a given electron pair are optimized self-consistently, they are typically found to be partially localized on the individual atoms comprising the bond. This is the case in Figure 2 and is particularly noticeable in parts A and B where the C–C $\sigma$-bond pairs are shown. Parts C and D show the pairs of orbitals that define the Ti–C bonds in the metallacycle. In each case one orbital appears essentially as an "$sp^3$ hybrid" on a carbon atom, and the remaining orbital shows predominantly 3d $\sigma$-bonding character. The 3d orbitals in Figure 2C,D are mixtures (hybrids) of the five atomic 3d orbitals. These hybrids both maximize orbital amplitude along the bond (and thus overlap with the carbon orbitals) and minimize overlap with each other. It is straightforward to show that the "best" (i.e., most directed) combination of atomic 3d orbitals producing a pair of $\sigma$-bonding orbitals would result in orbitals that are 55° apart.[15] The electron–electron and Pauli principle repulsions between two bonds that are 55° apart are large, however, and the presence of these

(14) Bobrowicz, F. W.; Goddard, W. A., III In "Modern Theoretical Chemistry: Methods of Electronic Structure Theory"; Schaefer, H. F., III, Ed.; Plenum Press: New York, 1977; Vol. 3, Chapter 4, pp 79–127.

(15) Pauling, L. "The Nature of the Chemical Bond"; Cornell University Press: Ithaca, NY, 1960; pp 151–152.

**Table II.** Summary of Geometric Parameters for the Olefin–Methylidene Complex

| center | $x$ | $y$ | $z$ |
|---|---|---|---|
| | (a) Atomic Coordinates (au) | | |
| Ti | −0.364 159 71 | −0.414 119 83 | 0.00 |
| Cl1 | 1.247 695 45 | −1.289 215 19 | −4.037 783 34 |
| Cl2 | 1.247 695 45 | −1.289 215 19 | 4.037 783 34 |
| C1 | −3.833 670 57 | −0.866 658 32 | 0.00 |
| C2 | −1.805 000 00 | 4.458 975 77 | 0.00 |
| C3 | 0.732 768 68 | 4.337 954 76 | 0.00 |
| H1 | −4.954 961 28 | −1.105 429 87 | −1.703 871 17 |
| H2 | −4.954 961 28 | −1.105 429 87 | 1.703 871 17 |
| H3 | −2.841 795 94 | 4.605 616 78 | −1.735 482 47 |
| H4 | −2.841 795 94 | 4.605 616 78 | 1.735 482 47 |
| H5 | 1.794 435 72 | 4.435 437 71 | −1.723 152 34 |
| H6 | 1.794 435 72 | 4.435 437 71 | 1.723 152 34 |

(b) Selected Bond Lengths (Å) and Angles (deg)

| | | | |
|---|---|---|---|
| $Ti-Cl_1,Cl_2$ | 2.35 | $C_1-C_3$ | 3.66 |
| $Ti-C_1$ | 1.85 | $C_2-C_3$ | 1.34 |
| $Ti-C_2$ | 2.69 | $C_1-H_1,H_2$ | 1.09 |
| $Ti-C_3$ | 2.58 | $C_2-H_3,H_4$ | 1.07 |
| $C_1-C_2$ | 3.02 | $C_3-H_5,H_6$ | 1.07 |
| $Ti-C_1-C_2$ | 61.7 | $H_3-C_2-H_4$ | 117.8 |
| $Ti-C_2-C_1$ | 37.3 | $H_5-C_3-H_6$ | 116.5 |
| $Ti-C_3-C_2$ | 79.7 | $Ti-C_1-H_1,H_2$ | 123.8 |
| $Ti-C_2-C_3$ | 70.8 | $C_2-C_3-H_5,H_6$ | 121.4 |
| $C_1-Ti-C_3$ | 110.4 | $C_3-C_2-H_3,H_4$ | 121.0 |
| $C_1-Ti-C_2$ | 81.0 | $Cl_1-Ti-Cl_2$ | 131.1 |
| $C_2-Ti-C_3$ | 29.5 | $Cl_1,Cl_2-Ti-C_1$ | 109.6 |
| $C_1-C_2-C_3$ | 108.1 | $Cl_1,Cl_2-Ti-C_2$ | 107.0 |
| $H_1-C_1-H_2$ | 112.1 | $Cl_1,Cl_2-Ti-C_3$ | 96.3 |

**Table III.** Summary of Geometric Parameters for the Transition-State Complex

| center | $x$ | $y$ | $z$ |
|---|---|---|---|
| | (a) Atomic Coordinates (au) | | |
| Ti | −0.345 648 83 | −0.87 767 90 | 0.00 |
| Cl1 | 1.425 302 84 | −1.229 877 37 | −3.968 772 63 |
| Cl2 | 1.425 302 84 | −1.229 877 37 | 3.968 772 63 |
| C1 | −3.824 167 65 | −0.843 334 10 | 0.00 |
| C2 | −2.296 748 69 | 4.199 105 02 | 0.00 |
| C3 | 0.262 063 51 | 4.148 889 65 | 0.00 |
| H1 | −4.973 418 97 | −0.946 707 41 | −1.697 968 21 |
| H2 | −4.973 418 97 | −0.946 707 41 | 1.697 968 21 |
| H3 | −3.348 991 26 | 4.375 606 93 | −1.722 085 01 |
| H4 | −3.348 991 26 | 4.375 606 93 | 1.722 085 01 |
| H5 | 1.311 098 46 | 4.329 348 68 | −1.729 977 36 |
| H6 | 1.311 098 46 | 4.329 348 68 | 1.729 977 36 |

(b) Selected Bond Lengths (Å) and Angles (deg)

| | | | |
|---|---|---|---|
| $Ti-Cl_1,Cl_2$ | 2.34 | $C_1-C_3$ | 3.41 |
| $Ti-C_1$ | 1.86 | $C_2-C_3$ | 1.35 |
| $Ti-C_2$ | 2.64 | $C_1H_1,H_2$ | 1.09 |
| $Ti-C_3$ | 2.42 | $C_2-H_3,H_4$ | 1.07 |
| $C_1-C_2$ | 2.79 | $C_3-H_5,H_6$ | 1.08 |
| $Ti-C_1-C_2$ | 65.7 | $H_3-C_2-H_4$ | 116.4 |
| $Ti-C_2-C_1$ | 39.9 | $H_5-C_3-H_6$ | 116.8 |
| $Ti-C_3-C_2$ | 83.5 | $Ti-C_1-H_1,H_2$ | 124.2 |
| $Ti-C_2-C_3$ | 65.8 | $C_2-C_3-H_5,H_6$ | 121.0 |
| $C_1-Ti-C_3$ | 105.1 | $C_3-C_2-H_3,H_4$ | 121.4 |
| $C_1-Ti-C_2$ | 74.4 | $Cl_1-Ti-Cl_2$ | 127.4 |
| $C_2-Ti-C_3$ | 30.7 | $Cl_1,Cl_2-Ti-C_1$ | 111.8 |
| $C_1-C_2-C_3$ | 105.7 | $Cl_1,Cl_2-Ti-C_2$ | 109.4 |
| $H_1-C_1-H_2$ | 111.6 | $Cl_1,Cl_2-Ti-C_3$ | 97.8 |

repulsions along with constraints of the ring geometry forces the bond angle to open up (in this case to 74.6°).

While the $C_1-Ti-C_3$ bond angle prefers to be small, the $Cl_1-Ti-Cl_2$ angle tends in the opposite direction for both the dichloro complexes treated here (133.5°), and though unreported for metallacyclobutane systems, dicyclopentadienyltitanium complexes in general have Cp–Ti–Cp angles around 130°.[16] As is well-known, bonds in both cases (Cl and Cp) are polarized strongly toward the ligands. We find these bonds to involve mostly 4s character at the Ti center. The bonds adopt a quasi-tetrahedral arrangement that minimizes repulsive interactions between these two polar bonds as well as steric interactions with the remainder of the complex. In a sense, a common function of the chloro and cyclopentadienyl ligands is to "remove" 4s electron density from the Ti atom and allow the formation of other shorter, highly directed bonds to the remaining (smaller) 3d orbitals.

**B. The Titanium Methylidene–Olefin Complex.** The product olefin–methylidene complex is shown schematically in Figure 1C, and geometric parameters are summarized in Table II. The carbon atoms and the titanium atom were constrained to be coplanar in the calculations. The dichlorotitanium methylidene moiety is only weakly perturbed by the presence of the olefin from the configuration found previously to be optimum for the isolated alkylidene complex.[12a] Principle differences arise from steric interactions between the chloride ligands and the olefin, as the chlorides bend substantially out of the titanium–methylidene plane. The methylene group is essentially undisturbed. The olefin seeks to reduce its interaction with the methylene group and assumes an asymetric orientation, with the $Ti-C_2$ distance 0.1 Å greater than the $Ti-C_3$ distance. Similarly, the angle subtended by the $C_1-Ti$ axis and the $C_3-Ti-C_2$ bisector is about 96°. The ethylene unit itself is very weakly perturbed: it is essentially planar, and all bond distances and angles depart only slightly from the corresponding gas-phase values.

Bonding orbitals for the system are shown in Figure 3. The olefin $\sigma$ bond (Figure 3B) is almost indistinguishable from the analogous gas-phase ethylene orbitals, and the $\pi$ bond (Figure 3A) is altered only by its small delocalization onto the Ti atom. As there are no filled d orbitals in this complex, the orbitals do not show "back-bonding" from the Ti into the antibonding olefin $\pi$ orbital that is characteristic of the Dewar–Chatt–Duncansen model for $\pi$ coordination.[17] This absence is further reflected both in the olefin C–C bond distance (1.34 Å) and the C–C stretching frequency (1542 $cm^{-1}$). The olefin coordination, in our view, arises from the donor–acceptor interaction between the filled olefin $\pi$ bond and partially occupied 3d (and 4s–4p) orbitals on the metal.

The titanium–methylene bonding interaction is essentially unchanged from that of the dichlorotitanium methylidene complex discussed elsewhere.[12a] The bond arises from metal–carbon $\pi$ and $\sigma$ bonds, shown in Figure, 3 parts C and D, respectively. The 3d occupation found on the Ti is thus $\sigma^1\pi^1$ ($3d_{x^2}{}^1 3d_{xy}{}^1$, in our coordinate system), rather than $\pi^2$ as suggested elsewhere.[18]

**C. Reaction Thermodynamics.** From differences in total energies of the reactants and products and the calculated vibrational frequencies, we estimate the thermodynamics of the isomerization reaction to be

$$Cl_2TiC_3H_6 \rightarrow Cl_2TiCH_2(C_2H_4)$$

$$\Delta H_{298} = 11.5 \text{ kcal/mol} \quad (2a)$$

$$\Delta S_{298} = 6.5 \text{ cal/(deg mol)} \quad (2b)$$

$$\Delta G_{298} = 9.6 \text{ kcal/mol} \quad (2c)$$

The relative stability of the metallacycle is consistent with the experimentally observed thermodynamic preference for the metallacycle in the dicyclopentadienyl analogue. Experimental studies of the dicyclopentadienyl analogues have focussed on the energetics of metathesis-related processes involving the metallacycle.[14] While these reactions were presumed to proceed through an olefin–titanium methylidene intermediate, no direct observation of such a species was noted. The absence of a barrier between the metallacycle and the $\pi$ complex in our results would suggest that isolation of the $\pi$ complex should be virtually impossible for a

(16) Petersen, J. L.; Dahl, L. F. *J. Am. Chem. Soc.* **1975**, *97*, 6422–6433.

(17) Dewar, M. J. S.; Ford, G. P. *J. Am. Chem. Soc.* **1979**, *101*, 783–791 and references therein.

(18) Eisenstein, O.; Hoffmann, R.; Rossi, A. R. *J. Am. Chem. Soc.* **1981**, *103*, 5582–5584.

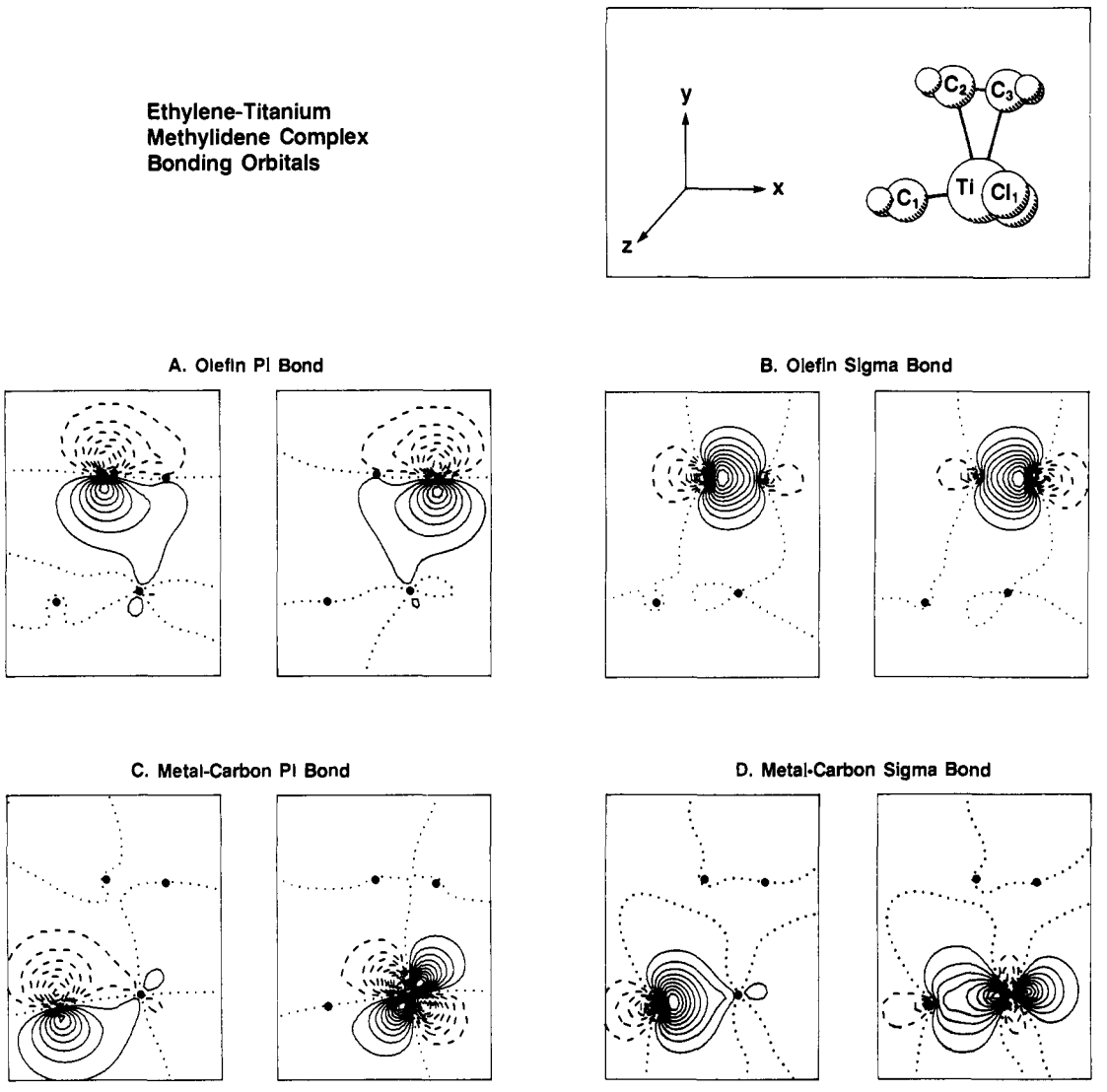


**Figure 3.** Contour plots of GVB orbitals defining both $\pi$ bonds in the ethylene–dichlorotitanium methylidene complex (A and C) as well as the $C_2$–$C_3$ and Ti–$C_1$ $\sigma$ bonds (B and D, respectively). The plotting plane contains the carbon and titanium atoms, and the figure is constructed analogously to Figure 2.

titanium system (this reaction coordinate is discussed further in section IIE).

**D. The Reaction Transition State.** Given the greater stability of the metallacycle, we would expect the transition state in the isomerization reaction to bear a resemblance to the olefin–methylidene complex, and indeed this is the case. The calculated transition state is shown schematically in Figure 1B, and its geometry is summarized in Table III. Once again, the carbon–titanium skeleton was constrained to be coplanar during the search for the transition state. The rationale here was that pronounced deviations from planarity are precluded by the strong steric interactions that would result with both the cyclopentadienyl ligands in the experimental system and the chloride ligands in our model system. The only major differences between the product and the transition state appear in the position of the olefin atoms. The angle between the $C_1$–Ti axis and the $C_3$–Ti–$C_2$ bisector decreases in the transition state to 90°, the $C_3$–Ti and $C_2$–$C_1$ distances are significantly shorter (by 0.16 and 0.22 Å, respectively, relative to the product), and the $C_2$–Ti and $C_1$–Ti distances shorten only slightly (by 0.05 and 0.01 Å, respectively, relative to the product).

**E. Reaction Coordinate.** The reaction coordinate involves both a rotation of the olefin center of mass about the Ti atom away from $C_1$ and a rotation of the olefin about its center of mass. The energy change along this coordinate possesses a negative second derivative, and calculated gradients in the energy at the geometry shown are zero (see Appendix), identifying this as a saddle point. In Figure 4, we show orbitals obtained from calculations proceeding approximately along the reaction coordinate from the metallacycle to the olefin–methylidene complex. Orbitals for this reactant (Figure 4A) and the product (Figure 4E) were taken from Figures 2 and 3, respectively. The atomic positions shown in the left column of Figure 4 correspond to the geometries used for the calculations producing the row of orbitals to the right of each molecular diagram. The orbitals have been arranged in such a way that the evolution of each orbital in the molecule that changes during the reaction may be followed by proceeding downward in a given column. Thus the orbitals that initially represented the Ti–$C_3$ and $C_1$–$C_2$ $\sigma$ bonds in the metallacycle evolve gradually to produce the Ti–$C_1$ and $C_2$–$C_3$ $\pi$ bonds in the product. It is of considerable importance to note the following: (1) Orbitals $C_2$ (column 2) and Ti (column 5) remain localized on $C_2$ and Ti, respectively, throughout the reaction. (2) Orbitals $C_3$ (column 4) and $C_1$ (column 3) exchange centers during the reaction. $C_1$ delocalizes through the $C_1$–$C_3$ bonding region without a node, while a node between $C_1$ and $C_3$ appears as $C_3$ delocalizes across this region.

As will be discussed in the next sections, this type of state evolution is to be expected and is responsible for the low barrier that occurs in this and related reactions. Most importantly, it is peculiar to reactions involving transition-metal centers and d orbitals in particular.

The transition-state energetic minimum found here lies only 2.3 kcal/mol above the olefin–methylidene complex and is essentially degenerate with it after the zero-point correction. The

activation barrier for conversion of the metallacycle to the olefin–methylidene complex is thus equivalent to the thermodynamic difference of 11.5 kcal/mol.

For the metathesis process, the metallacycle is presumed to open into the $\pi$ complex and subsequently exchange olefins as

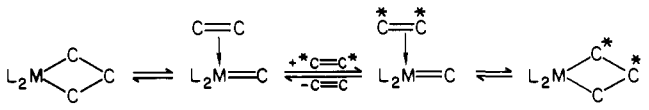

(3)

To address the kinetics of this reaction, we have also carried out calculations measuring the binding energy of the olefin in the $\pi$ complex,

$$Cl_2TiCH_2(C_2H_4) \rightarrow Cl_2TiCH_2 + C_2H_4 \qquad (4)$$

and obtain $\Delta H_{298}$ = 10.4 kcal/mol (see Figure 1D). From a straightforward analysis of the kinetics of the metathesis reaction, in which the $\pi$ complex and transition states in the metallacycle isomerization and olefin dissociation steps are assumed present in steady-state concentrations, we may conclude that the observed rate should reflect an activation enthalpy of approximately 21.9 kcal/mol (10.4 + 11.5 kcal/mol). Experimentally, the irreversible reaction of a *β-tert*-butyldicyclopentadienyltitanacyclobutane with diphenylacetylene has been found to possess an activation enthalpy of 26.9 kcal/mol,[13d] qualitatively consistent with the above result. The alternative explanation, that the measured activation energy is associated with a rate-limiting conversion of the metallacycle to the $\pi$ complex, may only be adopted if the barrier for the reverse reaction ($\pi$ complex to metallacycle) is similar in magnitude to the olefin binding energy (~10 kcal/mol). This interpretation is inconsistent with our calculated barrier (~0 kcal/mol) but leads to relative thermodynamic placements of the metallacycle and $\pi$ complex similar to those presented here (eq 2). It should be noted that an associative mechanism (where both olefins are bound to the alkylidene complex) would be possible for our coordinatively unsaturated dichloro complex (the bis(olefin) complex would be a 12-electron system) and in fact would have a barrier lower than the dissociative mechanism described above (~10 kcal/mol lower). This associative mechanism is not likely for the experimental dicyclopentadienyl system as the bis(olefin) complex would be a 20-electron system (barring cyclopentadienyl ring slippage).

**F. Previous Theoretical Studies of the Barrier in Olefin Metathesis.** Hoffmann and co-workers[18] have studied the olefin metathesis reaction pathway using the extended Hückel method. The set of complexes they examined included $Cp_2Ti(CH_2)(C_2H_4)$, for which they obtained results diametrically opposed to other theoretical work,[12] experiment,[13] and the work reported here. Specifically, they find the metallacyclobutane substantially less stable than the olefin–methylidene complex (by approximately 20 kcal/mol). Further, they find the global potential energy surface minimum to be associated with a geometry close to that found here for the saddle point. This minimum was found to be approximately 6 kcal/mol below the olefin–methylidene complex. A point of agreement common to our work, experiment, and the work of Hoffmann and co-workers is that the observed barrier should be small.

## III. Theoretical Concepts: Barriers to Exchange Reactions

In this section, we briefly review the concepts needed to understand the manner in which reactant electronic states may evolve continuously into product states and how the details of the process determine the reaction energetics. We consider exchange reactions for which the bond order (two) remains unchanged (there may be other bonds in the system that do not participate). This class of reactions includes an enormous array of processes, ranging from simple $H_2 + D_2$ exchange to dissociative adsorption on metal surfaces and transition-metal reactions such as olefin insertions, polymerizations, and reductive eliminations. The prototypical metathesis reaction being considered here is also an example of such a process. Each of these reactions is formally a 2 + 2 process and thus Woodward–Hoffmann forbidden.[5] Restrictions imposed upon these processes by the Pauli principle and spin conservation lead to large barriers in simple organic exchange reactions.[5-11] We show below, however, that in many cases these same constraints allow much smaller barriers when a transition-metal center is involved.

The basis for the theory underlying these claims appears in part in a number of references[11] and has recently been recast in a form relevant to the study of barriers in surface reactions,[10] and thus need not be repeated here in detail. Below, we discuss the forbidden coplanar ethylene plus ethylene to cyclobutane transformation and contrast its properties with a transition-metal-assisted analogue. Finally, we relate the discussion to the low-barrier titanium complex isomerization process.

**A. Pauli Principle Constraints on Exchange Reactions.** We consider first the process of forming cyclobutane via the coplanar exchange reaction $2C_2H_4 \rightarrow C_4H_8$. This reaction is useful for illustrating how the constraints of the Pauli principle determine the evolution of one-electron states from reactants to the transition state in a reaction where $\pi$ orbitals are involved.[11] We presume the reaction to begin from an interaction geometry in which the ethylene C–C bonds are parallel to one another and the C–H bonds extend out of the reaction plane. The reaction limit wave functions may be represented as

$$\Psi(C_2H_4 + C_2H_4) = {}^1A_{1g} = \mathcal{A}\{\pi_2\pi_3(\alpha\beta - \beta\alpha)\pi_1\pi_4(\alpha\beta - \beta\alpha)\} \qquad (5a)$$

$$\Psi(C_4H_8) = {}^1A_{1g} = \mathcal{A}\{\sigma_2\sigma_1(\alpha\beta - \beta\alpha)\sigma_3\sigma_4(\alpha\beta - \beta\alpha)\} \qquad (5b)$$

where the subscripts identify the atomic locations of the orbitals. The $\pi_i$ orbitals are 2p orbitals on the olefin carbons that are coupled into a singlet (bond) to produce an olefin $\pi$ bond. Orbitals $\sigma_i$ are "$sp^3$"-like hybrids and are singlet coupled to form product $\sigma$ bonds. For the geometry chosen here, bonds are formed between the first two and last two orbitals listed in each wave function. For the total wave function to be an eigenfunction of spin, each of the first two orbitals is then coupled to each of the last two orbitals via a predominantly triplet ($^3/_4$ triplet + $^1/_4$ singlet) or "antibonding" interaction. A schematic display of these interactions and the orbital positions is as follows:

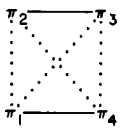

(6a)

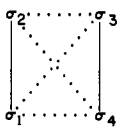

(6b)

In eq 6, the solid line represents a singlet coupling between the orbitals connected by it, and the sparse dotted line denotes the partial triplet coupling. In eq 6, the solid line represents a singlet coupling between the orbitals connected by it, and the sparse dotted line denotes the partial triplet coupling. The Pauli principle, in requiring a wave function of the form shown in eq 5, allows two "bonding" interactions in each wave function (the solid lines) and necessitates two additional partial "antibonding" interactions (the dotted lines). The "antibonding" interactions vanish as the molecule–molecule separation increases.

As the atoms move from either reactant or product position to the transition state, the four carbon atoms form a rectangle. The reactant (eq 5a) and product (eq 5b) states are similar in energy at this point, but neither is appropriate to accurately describe the transition-state wave function. It may be approximately represented as a superposition of these two states

$$\Psi(TS)_\pm = N_\pm\{\Psi(C_2H_4 + C_2H_4) \pm \Psi(C_4H_8)\} \qquad (7)$$

$$+ \text{ sign (7a); } - \text{ sign (7b)}$$

where $N_\pm$ is the appropriate normalization and the two possible states correspond to symmetric or antisymmetric superposition. A more complete expression would include ionic contributions,[10,11]

but for this qualitative description the above is sufficient. Interactions in these two wave functions become (using reactant orbital designations)

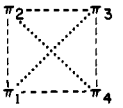


(8a)

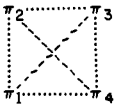


(8b)

Two orbitals that are triplet coupled are connected by the dotted lines. The remaining pairs of orbitals are primarily singlet coupled and are connected to each other by dashed lines, $\Psi_+$ (eq 8a) maximizes the separation between triplet-coupled orbitals while maximizing the overlap between partially singlet-coupled (bonding) orbitals and is thus preferred over $\Psi_-$ where the reverse occurs. The lowest transition state wave function will be best represented by the symmetric superposition, $\Psi_+$. It provides the best opportunity to maintain bond order. The appearance of a low-energy transition state (i.e., small barrier) will be largely a result of how well these specific orbitals are able to maximize the strength of the "bonding" interactions while minimizing the destabilization resulting from triplet interactions.

In the approach toward the transition state the four one-electron orbitals delocalize onto different centers.[10,11] We illustrate this process in Figure 5. The figure is constructed in the same way as Figure 4, with each row defining a stage in the reaction and each column monitoring the evolution of a particular orbital during the reaction. Columns 2 and 3 of Figure 4E and columns 1 and 2 of Figure 5A both define the bonding $\pi$ orbitals of an olefin unit. Columns 3 and 4 show the $\pi$ bond of the second olefin in Figure 5A.

The driving force for delocalization is the presence of triplet interactions in the transition-state wave function (dense dotted lines in eq 8a). These are repulsive interactions, and the Pauli principle forces the pair of orbitals involved in each interaction (connected by the dotted lines) to become orthogonal to one another. This orthogonality requirement is the most important effect of the superposition process and the source of the energetic barrier. This orthogonality condition is best satisified by the formation of delocalized bonding–antibonding orbital pairs. Thus orbital $\pi_3$ delocalizes across to center $C_1$ with a change in phase to form a half-filled bonding "$\sigma$" orbital (henceforth called $\sigma_{13b}$), while $\pi_1$ delocalizes back across to form a half-filled antibonding "$\sigma$" orbital ($\sigma_{13a}$). A similar adjustment occurs for $\pi_2$ and $\pi_4$ leading to new orbitals $\sigma_{24b}$ and $\sigma_{24a}$. This is illustrated in Figure 5B.

In terms of these new delocalized orbitals, the transition-state wave function $\Psi_+$ becomes

$$\Psi_+ = \{(\sigma_{13b}\sigma_{24b})(\alpha\beta - \alpha\beta)(\sigma_{13a}\sigma_{24a})(\alpha\beta - \beta\alpha)\} \quad (9)$$

This wave function is analogous to eq 5 in which the delocalized half-filled bonding orbitals $\sigma_{13b}$ and $\sigma_{24b}$ are singlet coupled, as are the two antibonding orbitals. Figure 5B reflects this orbital pairing. The energetic position of the transition state hinges upon the strength of the bonds between the delocalized orbitals. The bonding orbitals $\sigma_{13b}$ and $\sigma_{24b}$ overlap substantially, as may be seen in Figure 5B.

The antibonding orbitals $\sigma_{13a}$ and $\sigma_{24a}$, on the other hand, are almost orthogonal to each other (cf. Figure 5B). As a result, the bond between them in $\Psi_+$ has little strength. In effect, the bond order of the transition state is reduced to one. The large barrier in this reaction is a result of the orbital evolution that occurs on going to the transition state: orbital orthogonality requirements lead to four delocalized orbitals, only two of which overlap to produce a bond. The energy of the transition state is high, and the reaction is forbidden.

**B. A Transition-Metal Analogue: The Metallacyclobutane Formation Reaction.** The analysis of the coplanar addition of two ethylene monomers to produce cyclobutane has a transition-metal analogue in the formation of a metallacycle from an olefin and a metal alkylidene

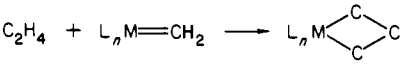


(10)

For the most part it is the local symmetries of the orbitals that change: we are still concerned with the evolution of two $\pi$ bonds in the reactants to two $\sigma$ bonds in the product. In this case, one of the olefin $\pi$ bonds is replaced by a metal–alkylidene $\pi$ bond in the reactants, and two carbon–carbon $\sigma$ bonds are replaced by metal–carbon bonds in the products. The wave functions and energetic interacitons used above (eq 5–8) are transferable directly to this problem with only a change in notation. The initial- and final-state wave functions are

$$\Psi(\text{alkylidene + ethylene}) = \{\pi_2\pi_3(\alpha\beta - \beta\alpha)\pi_1 d\pi_4(\alpha\beta - \beta\alpha)\} \quad (11a)$$

$$\Psi(\text{metallacycle}) = \{\sigma_2\sigma_1(\alpha\beta - \beta\alpha)\sigma_3 d\sigma_4(\alpha\beta - \beta\alpha)\} \quad (11b)$$

Here, $d\pi_4$ and $d\sigma_4$ are the metal $3d_\pi$ and $3d_\sigma$ orbitals of the reactant alkylidene and product metallacycle, respectively. They replace the corresponding 2p $\pi$ and $\sigma$ carbon orbitals in eq 5. The transition state possesses low symmetry, but its behavior may be understood as before if it is represented approximately as a superposition of the initial- and final-state wave functions. The symmetric superposition is again lowest in energy, and it may be schematically represented as

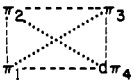


(12)

where as before the initial-state notation is retained. As in cyclobutane formation, the state evolution is determined by the presence of the triplet interactions in the transition-state wave function. This evolution is illustrated in Figure 6. Orthogonality constraints exist again, so $\pi_3$ and $\pi_1$ will form a bonding–antibonding orbital pair delocalized over $C_3$ and $C_1$. The localized orbitals $\pi_2$ and $d\pi_4$ (labeled M in Figure 6) are already almost orthogonal, and only minor adjustments are needed in order to satisfy the Pauli principle orthogonality requirement. Expressing the transition-state wave function $\Psi_+$ in terms of this new set of orbitals leads to (see Appendix)

$$\Psi_+ = \{(\sigma_{13b}\pi_2)(\alpha\beta - \beta\alpha)(\sigma_{13a}d\pi_4)(\alpha\beta - \beta\alpha)\} \quad (13)$$

This expression is similar to eq 9 in that the transition-state orbitals are combined into two bonding combinations. There are, however, important differences between this wave function and that which was found to dominate in the cyclobutane case. In this case, $\Psi_+$ contains two bonds: one between $\sigma_{13b}$ and $\pi_2$ and another between $\sigma_{13a}$ and $d\pi_4$. The first of these involves orbitals that overlap well (Figure 6B), and as before a strong bond would be expected. Unlike the previous situation, the second bond also contains orbitals that overlap well since the change in sign of the antibonding $\sigma_{13a}$ orbital matches the change in sign of the $3d\pi$ orbital. As a result, *two* bonds are retained in the transition state here, and we would expect a transition state of low energy. We find that the presence of the different local orbital character of the $3d\pi$ orbital allows satisfaction of the Pauli principle orthogonality requirement without disruption of the second strong covalent bond in the transition state. The wave function is able to move smoothly from reactants through the transition state to the products without a change in the degree of covalent bonding. This is in sharp contrast to what occurs when the d orbital is absent: the Pauli principle requirement leads to a loss of bonding in the transition state.

While the difference in orbital shapes and overlaps that distinguish the two reactions may seem trivial, we have shown that the interactions defined by the *form* of the wave function determine how the states will continuously evolve in the reaction. The evolution cannot always occur smoothly, as it is tempting to assume, because of the Pauli principle restrictions. It is appealing to recognize that the enormous differences in the energetic evo-

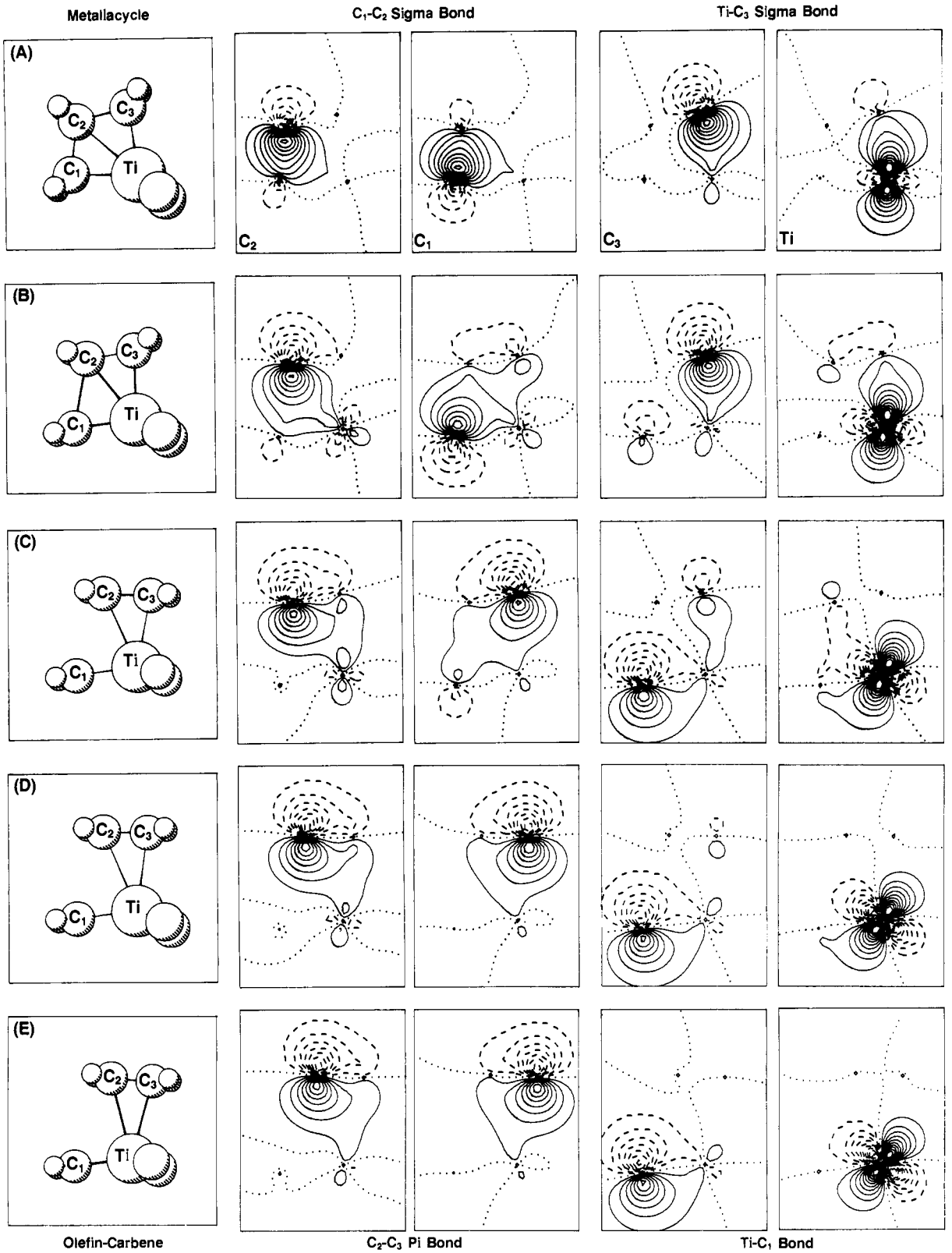


**Figure 4.** The evolution of the parent metallacycle to the product olefin–carbene complex, as reflected in selected ring skeleton bonding orbitals. Each row depicts a stage in the transformation: column 1 shows the molecular geometries, with atoms in the orbital plotting plane labeled; columns 2 and 3 show the evolution of the initial $C_1$–$C_2$ $\sigma$ bond to the final $C_2$–$C_3$ $\pi$ bond in terms of a pair of one-electron GVB orbitals; columns four and five show the evolution of the Ti–$C_3$ $\sigma$ bond to the product Ti–$C_1$ $\pi$ bond. The remaining Ti–$C_1$ and $C_2$–$C_3$ $\sigma$ bonds do not change character and are not shown. Contours are defined as in Figures 2 and 3.

lution of these fairly complex reactions may be reduced to the observation of a simple, clearly identifiable difference in the orbital nodal structure.

**C. The Titanium Metallacycle to Carbene–Olefin Isomerization.** The discussion above was devoted to the metallacycle formation reaction in order to easily draw comparisons with the simpler and more familiar organic analogue. The reaction being considered through detailed calculations in section II, and depicted in Figure 4, is just the reverse of this process. This figure may now be reexamined in light of the above discussion.

The most important orbital changes in Figure 4 are those in columns 3 and 4, where the evolution from $\sigma$-bonding orbitals to

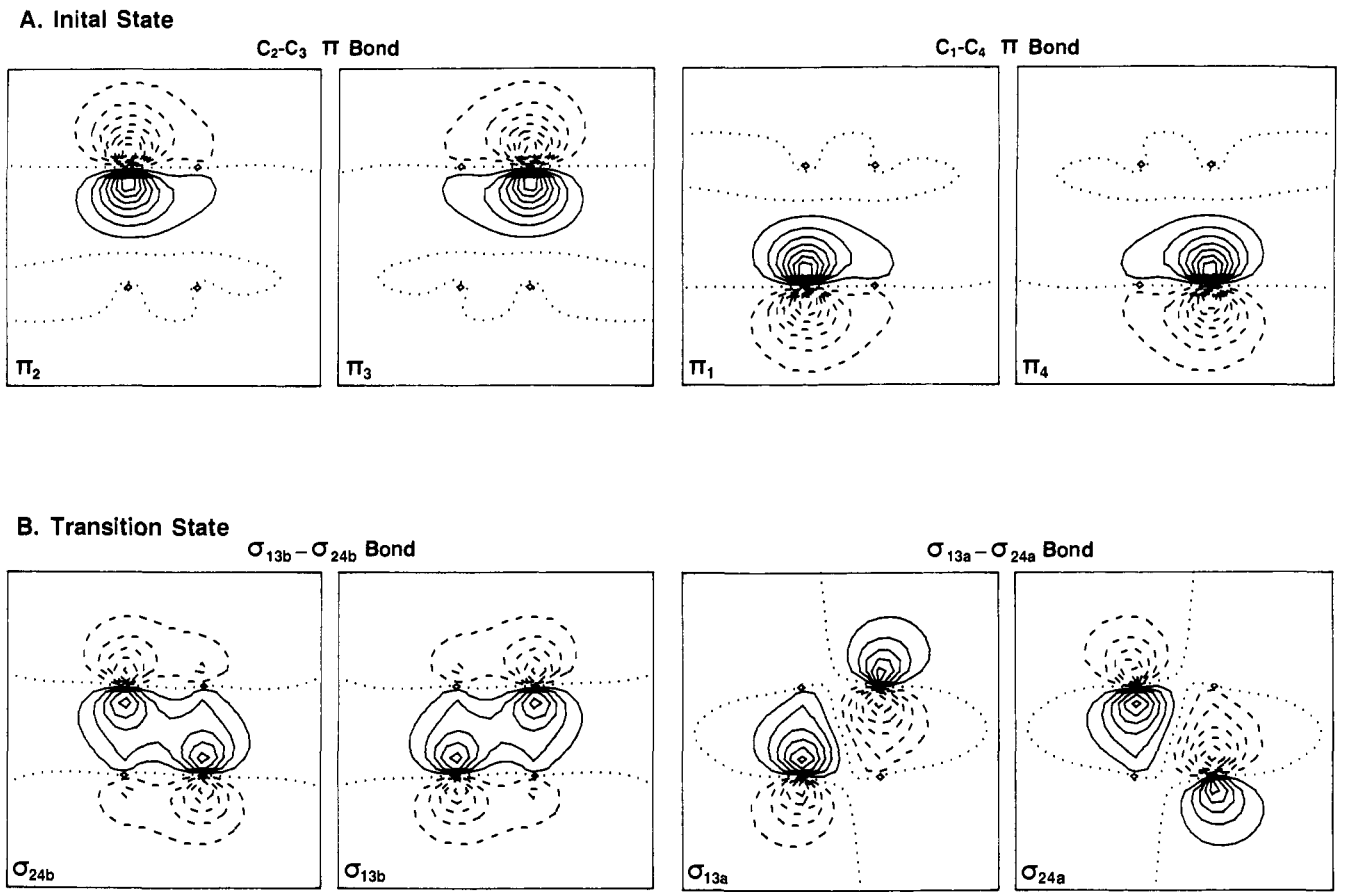


**Figure 5.** A schematic of the $\pi$-bonding orbital evolution that occurs in the olefin → cyclobutane transformation. Columns 1, 2 and 3, 4 show pairs of singlet-coupled GVB orbitals. Row A shows the initial olefin $\pi$-bond character of these pairs, while row B indicates how each orbital has delocalized upon entering the transition state.

olefin and alkylidene $\pi$ orbitals occurs. The $C_1$ orbital (column 3) in Figure 4B,C delocalizes across to center $C_3$ to form a bonding orbital and by Figure 4D is localized on $C_3$ as one component of the product olefin $\pi$ orbital. The $C_3$ orbital of Figure 4A (column 4) delocalizes to center $C_1$ in Figure 4B,C to form an antibonding orbital, and in Figure 4D it has localized as the carbon 2p component of the alkylidene $\pi$ orbital. Similarly, we see that the Ti orbital (Figure 4, column 5) evolves from a 3d$\sigma$ orbital in Figure 4A toward a 3d$\pi$ orbital in Figure 4B,C in order to retain the overlap with the antibonding $C_3$ orbital, the predicted source of the low barrier. It remains mostly localized on the Ti atom and is clearly orthogonal in Figure 4C to the orbitals in columns 2 and 3. Orbitals $C_1$ and $C_2$ also clearly retain strong overlap in Figure 4B,C as needed. These orbital evolutions are simply the reverse of those described in the last section.

The detailed calculations provide an opportunity to see the complete evolution from reactants to products. Figure 4B,C corresponds approximately to the position of the transition state. The bonding–antibonding combination of orbitals predicted is seen to be present in these detailed calculations. The antibonding (triplet) interactions are minimized, while all bonding interactions are retained. In effect, each of the individual reactant bonds simply shifts to the product positions without disruption. It is tempting to assume that all 2 + 2 exchange reactions might occur this way, but as we have shown, the Pauli principle introduces restrictions that make this impossible in most cases. As expected, the energetic evolution during this reaction reflects mostly the changes in individual bond strengths: except for the very small energetic barrier near the olefin–methylidene complex (Figure 4) the energy rises smoothly from the more stable metallacycle to the product.

## IV. Discussion: Extension to General Carbon–Carbon, Metal–Ligand $\pi$-Bonded Systems

Our results suggest that in general (given thermodynamic accessibility) 2 + 2 4$\pi$ electron reactions where one of the component electrons is in a d orbital will occur with very small kinetic barriers. Below we will discuss specific examples of several such processes.

**A. Olefin Metathesis.** The extention of the above results to olefin metathesis in general

$$R'_2C{=}CR'_2 + R_2C{=}CR_2 \rightarrow 2R'_2C{=}CR_2 \qquad (14)$$

is straightforward. The generally accepted mechanism for olefin metathesis[1] involves the reaction of a metal alkylidene with an olefin to form a metallacyclobutane which then decomposes to generate a new olefin and a new alkylidene complex.

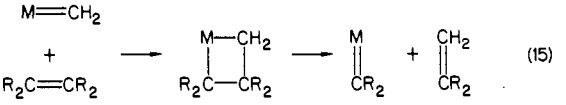


(15)

As discussed in section II we find this process to have a very low kinetic barrier. As noted previously[12a,13] the difficulty for titanium systems is the thermodynamic instability of titanium methylidene complexes. For Cr, Mo, and W tetrachloride systems it has previously been demonstrated that alkylidene complexes are the thermodynamic sink.[19] Further, for Cr, Mo, and W oxo dichloride methylidene systems, with appropriate cocatalysts, the thermodynamics are balanced.[19] The reasoning outlined in section III suggests that these Cr, Mo, and W oxo systems will be quite active catalysts with small kinetic and thermodynamic barriers. The experimental evidence from the Schrock group[20] is in agreement with this suggestion.

(19) Rappé, A. K.; Goddard, W. A., III *J. Am. Chem. Soc.* **1982**, *104*, 448–456.

(20) Schrock, R. R.; Rocklage, S.; Wengrovious, J.; Rupprecht, G.; Fellmann, J. *J. Mol. Catal.* **1980**, *8*, 73–83. Wengrovious, J. H.; Schrock, R. R.; Churchill, M. R.; Missert, J. R.; Youngs, W. J. *J. Am. Chem. Soc.* **1980**, *102*, 4515–4516.

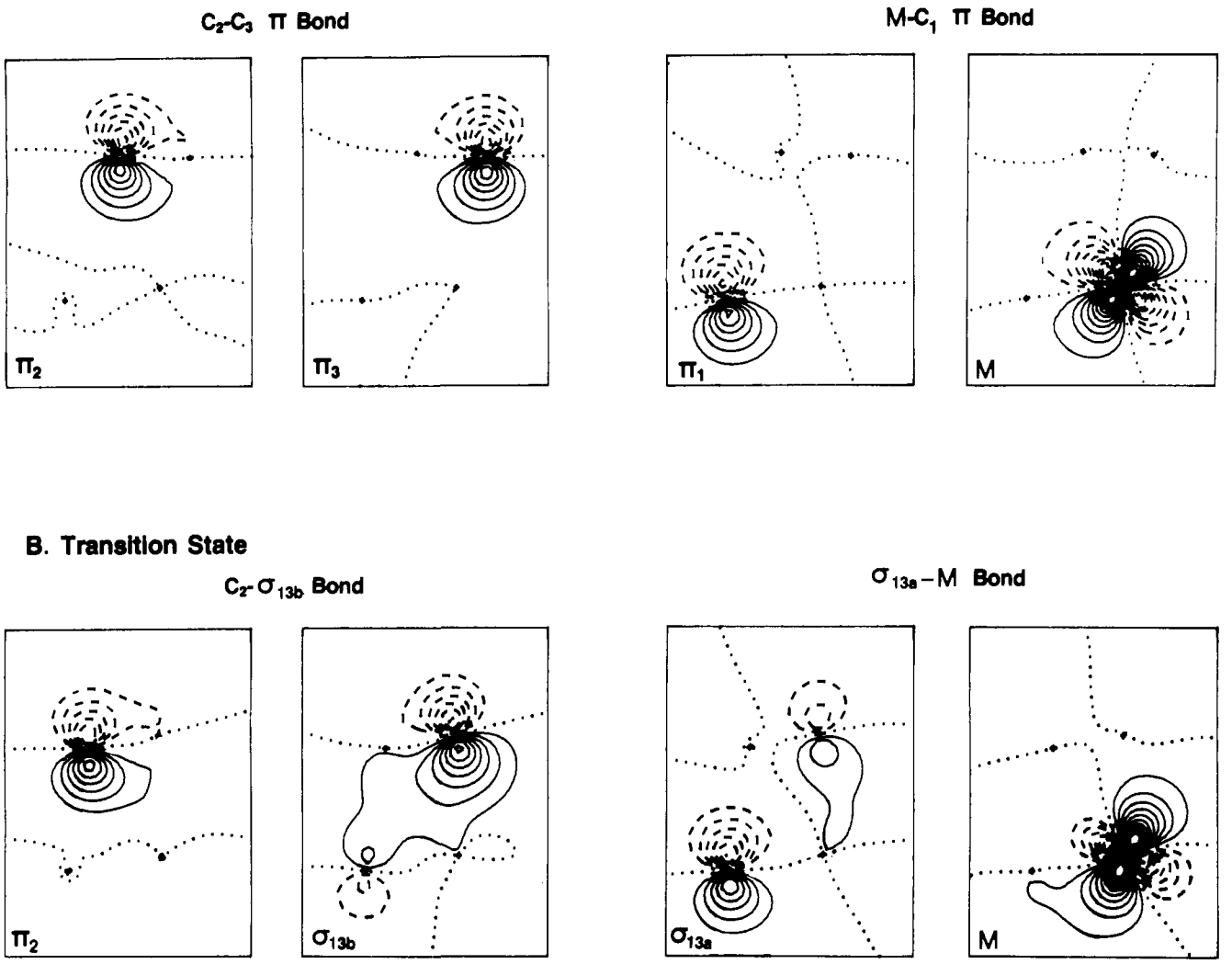


**Figure 6.** An analogue to the process depicted in Figure 5 in which an olefin and a carbene combine to form the metallacycle. Row A depicts the initial olefin and carbene $\pi$-bond GVB orbitals, while row B shows the delocalization that occurs upon entering the transition state.

**B. Acetylene Metathesis.** The process analogous to eq 14 for acetylenes

$$R'C{\equiv}CR' + RC{\equiv}CR \rightarrow 2R'C{\equiv}CR \qquad (16)$$

has only recently been systematically studied.[2] Schrock and co-workers[2f-i] have found that tungsten alkylidyne complexes such as $W(CCMe_3)(OCMe_3)_3$ will catalyze the metathesis of acetylenes, and they concur with Katz's suggestion[2e] that acetylene metathesis is likely to occur through the intermediacy of a metallacyclobutadiene.

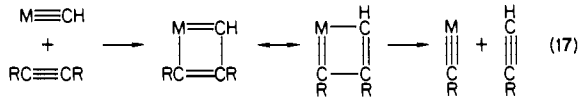


The intermediacy of such metallacycles is supported by a crystal structure of $W[C\text{-}t\text{-}BuCMeCMe]Cl_3$.[2i] This process is analogous to olefin metathesis in that a metal–carbon $\pi$ bond is adding across a carbon–carbon $\pi$ bond. We suggest that this process has a low kinetic barrier for exactly the same reasons as for olefin metathesis.

**C. Olefin Oxidation.** Extension of the energetics and concepts discussed above to metal–oxo complex olefin oxidation provides "kinetic" support for a controversial mechanism originally proposed by Sharpless and co-workers[21] for chromyl chloride oxidation of olefins.

The classic mechanism[22] for polyoxo oxidation consists of a simple concerted addition of the olefin $\pi$ bond across two metal–oxo bonds,

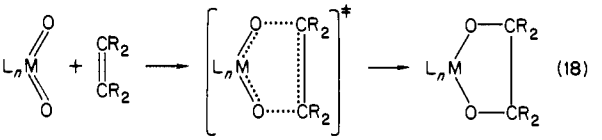


The alternate Sharpless mechanism was formulated to explain the observation that chromyl chloride oxidation of olefins does not produce cis diols as would be expected from eq 18. Chromyl chloride instead forms epoxides and cis hydrochlorins. The proposed mechanism consists of an initial 2 + 2 reaction of the olefin across the metal–oxygen $\pi$ bond forming a metallacyclooxetane which has various reductive elimination pathways available (eq 19). The first two products (eq 19a and 19b) have been shown[23] to be energetically accessible, whereas the third (reductive elimination) product (eq 19c) is not thermally accessible. As before, our results suggest that the alternate Sharpless mechanism should in fact occur easily; the addition of an olefin $\pi$ bond across a metal–oxygen $\pi$ bond should occur kinetically as readily as the

(21) Sharpless, K. B.; Ternanishi, A. Y.; Backvall, J. E. *J. Am. Chem. Soc.* **1977**, *99*, 3120–3128.

(22) Schroder, M. *Chem. Rev.* **1980**, *80*, 107–213. Schroder, M.; Constable, E. C. *J. Chem. Soc., Chem. Commun.* **1982**, 734–736. Casey, C. P. *Ibid.* **1983**, 126–127.

(23) Rappé, A. K.; Goddard, W. A., III *J. Am. Chem. Soc.* **1982**, *104*, 3287–3294.

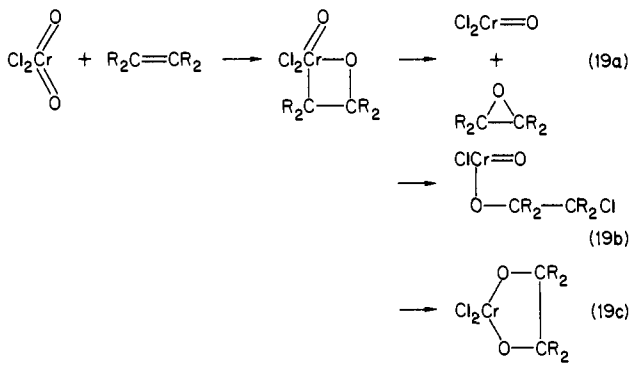

addition across a metal–carbon $\pi$ bond.

We suggest that the same mechanism is operative for $OsO_4$. In this case the osmate ester is the only possible reductive elimination product and is apparently thermally accessible for osmium. This observation is straightforwardly extended to $RuO_4$ and $MnO_4^-$ oxidations, which also form cis diols exclusively.

**D. Olefin Polymerization.** Ziegler–Natta olefin polymerization, despite being a major industrial process, is not understood at a molecular level. Two mechanisms for this reaction are consistent with the available experimental data. The first, proposed by Cossee and Arlman,[24] consists simply of an addition of a metal–carbon $\sigma$ bond across a carbon–carbon $\pi$ bond of a coordinated olefin.

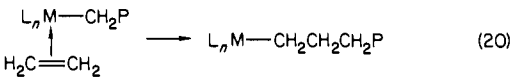

This is the generally accepted mechanism and has recently received mechanistic support through the work of Watson[4f] where direct olefin insertion into a lutetium–carbon bond was observed. The alternant mechanism, proposed by Rooney, Green, and co-workers,[4e] starts with the metal alkyl complex, but prior to olefin insertion a 1,2-hydrogen shift occurs, generating a metal alkylidene hydride complex that reacts with the olefin to generate a metallacyclobutane hydride complex. Completing the reaction the metallacyclobutane hydride reductively eliminates generating a metal alkyl that has been chain extended.

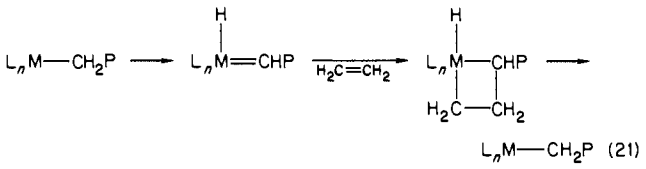

This mechanism has also received experimental support recently. Schrock and co-workers[4g,j] have demonstrated that a stable alkylidene hydride complex, $Ta(CHCMe_3)(H)(PMe_3)_3I_2$, will polymerize olefins; the only identifiable complex in solution is the alkylidene hydride.

The extension of our work to the Rooney–Green mechanism is straightforward. If the rate-limiting step is an olefin insertion across a metal–carbon $\pi$ bond, our energetics and the associated conceptual framework are directly applicable. Thus, we suggest that eq 21 will occur quite easily. Schrock and co-workers[4j] have also demonstrated using proton NMR saturation transfer that the 1,2-shift occurs faster than net chain extention.

Our results can also be extended to the Cossee–Arlman mechanism as the addition across a metal–carbon $\sigma$ bond will also have the appropriate nodal structure to permit a low electronic barrier. However, the "steric congestion" associated with a direct addition across a metal–"$sp^3$" carbon bond obviates activation energies as low as 6 kcal/mol for eq 20. We have found[25] the barrier for addition of ethylene across the Ti–C $\sigma$ bond of $Cl_3Ti–CH_3$ to be greater than 25 kcal/mol. This congestion prevents the direct insertion from occurring at a rapid enough rate to be competitive with an insertion across a metal–carbon $\pi$ bond. Further, we assert that the metal/ligand system must be providing such an avenue for titanium catalytic systems.[4i]

**E. Transition-Metal-Assisted Formation of 1,2-Dinitrosoalkanes.** To extrapolate our results to nitrogen systems, we consider the reaction of a cobalt dinitrosyl complex with an olefin to generate a complexed 1,2-dinitrosoalkane.

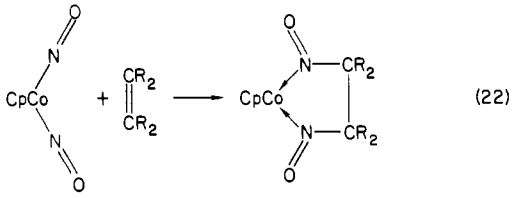

This reaction was originally reported by Brunner and co-workers,[26] and the scope and mechanism was subsequently investigated by Bergman and co-workers.[27] Bergman has concluded that the reaction proceeds by a concerted addition across both nitrosyl $\pi$ bonds in analogy to the classical mechanism for osmium tetraoxide olefin oxidation[22] (an alternant mechanistic possibility for this reaction was discussed above). We feel that a more plausible reaction sequence involves the concerted addition of a single metal–nitrogen $\pi$ bond across the olefin $\pi$ bond. This is followed by a rapid reductive elimination involving the second metal–nitrogen $\pi$ bond to form the observed 1,2-dinitrosoalkane.

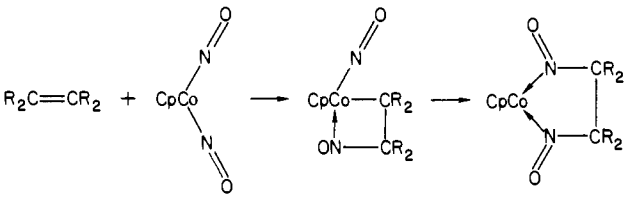

The mechanistic sequence in eq 23 is preferable; we have demonstrated (and provided an explanation for the observation) that the addition of an olefin across a metal–ligand $\pi$ bond will occur with a small barrier (on the order of 2 kcal/mol). Further, reductive elimination reactions are well-known in organometallic chemistry[28] and are documented to occur with small kinetic barriers.[29]

## Appendix: Calculational Details

**A. Basis Sets and Effective Potentials.** All of the calculations reported here were carried out by using Cartesian Gaussian basis sets. For both Cl[30] and Ti, an effective potential was used to replace the core electrons, allowing self-consistent orbital optimization to be carried out only for the valence electrons. For geometry optimizations a (7s,4p/3s,2p) basis was used for carbon,[31] and a (4s/2s) basis for hydrogen.[32] The carbon basis was

(24) Cossee, P. *J. Catal.* **1964**, *3*, 80–88. Arlman, E. *Ibid.* **1964**, *3*, 89–98. Arlman, E. J.; Cossee, P. *Ibid.* **1964**, *3*, 99–104.

(25) Rappé, A. K.; Upton, T. H. "Abstracts of Papers", 185th National Meeting of the American Chemical Society, Seattle, WA, March 1983; American Chemical Society: Washington, DC, 1983; INOR 301.

(26) Brunner, H. *J. Organomet. Chem.* **1968**, *12*, 517–522. Brunner, H.; Loskot, S. *Ibid.* **1973**, *61*, 401–414.

(27) Becker, P. N.; White, M. A.; Bergman, R. G. *J. Am. Chem. Soc.* **1980**, *102*, 4676–5677. Becker, P. N.; Bergman, R. G. *Ibid.* **1983**, *105*, 2985–2995.

(28) Collman, J. P.; Hegedus, L. S. "Principles and Applications of Organotransition Metal Chemistry"; University Science Books; Mill Valley, CA, 1980.

(29) Norton, J. R. *Acc. Chem. Res.* **1979**, *12*, 139–145 and references within.

(30) Rappé, A. K.; Smedley, T. A.; Goddard, W. A., III *J. Phys. Chem.* **1981**, *85*, 1662–1666.

(31) Rappé, A. K.; Goddard, W. ., III In "Potential Energy Surfaces and Dynamics Calculations"; Truhlar, D. G., Ed.; Plenum Press: New York, 1981; pp 661–684.

(32) Dunning, T., Jr.; Hay, P. J. In "Modern Theoretical Chemistry: Methods of Electronic Structure Theory"; Schaefer, H. F., III, Ed.; Plenum Press: New York, 1977; Vol. 3, Chapter 1, p 1.

**Table IV.** Terms of the Ti Atom Ar Core Potential

| $l$ | $n_i$ | $d_i$ | $c_i$ |
|---|---|---|---|
| | | Unprojected ($l_{max}$) Terms[a] | |
| 3 | −1.0 | 0.638 528 28 | 0.745 761 46 |
| 3 | −1.0 | 0.979 107 64 | −4.445 449 1 |
| 3 | −1.0 | 3.544 724 5 | −3.065 743 4 |
| 3 | −1.0 | 22.022 970 | −6.291 431 1 |
| | | Projected Terms[a] | |
| 0 | −2.0 | 19.659 314 | 4.011 483 4 |
| 0 | 0.0 | 15.429 894 | 85.135 915 |
| 0 | 0.0 | 4.031 415 7 | 37.926 207 |
| 0 | 0.0 | 0.923 114 04 | 11.348 900 |
| 1 | −2.0 | 5.737 639 1 | 6.416 237 3 |
| 1 | 0.0 | 5.153 381 6 | 30.579 369 |
| 1 | 0.0 | 1.763 756 3 | 19.391 560 |
| 1 | 0.0 | 0.556 414 70 | 4.046 193 9 |
| 2 | 0.0 | 0.977 080 24 | 1.038 680 4 |
| 2 | 0.0 | 0.603 870 84 | −0.765 341 96 |
| 2 | 0.0 | 0.297 893 63 | −0.174 485 59 |
| 2 | 0.0 | 10.818 483 | −1.871 838 4 |

[a] Potential is of the form

$$V = V(l_{max}) + \sum_{l=0}^{l_{max}-1} \{V(l) - V(l_{max})\}|l\rangle\langle l|$$

where $V(l) = \sum_i c_i r^{n_i} exp(d_i r^2)$.

augmented with a single set of d Gaussians ($\zeta = 0.75$) for a final set of calculations at the optimum geometries. For chlorine a valence minimum basis (3s,3p/1s,1p)[31] was used. For Ti, the core potential was obtained by using the method of Kahn,[33] the terms of which are listed in Table IV. A valence double $\zeta$ (3s,2p,4d/2s,2p,2d) basis[31] was used with this potential.

**B. Wave Functions.** Both Hartree–Fock (HF) and generalized valence bond (GVB)[14] wave functions were obtained during each step in the geometry optimization procedure (see below). The generalized valence-bond wave function introduces important electron pair correlation effects by allowing each electron in a valence electron pair to have its own orbital. For a filled olefin $\pi$ orbital, for example, this appears as

$$\phi(\text{olefin } \pi) = \{(\lambda_u\pi_u^2 - \lambda_g\pi_g^2)(\alpha\beta - \beta\alpha)\} = \{(\pi_1\pi_2 + \pi_2\pi_1)(\alpha\beta - \beta\alpha)\} \quad \text{(A1)}$$

where the $\pi_i$ ($i = 1, 2$) are orbitals essentially localized on individual carbon centers (see Figure 5). These $\pi_i$ are allowed to be completely general (i.e., delocalized if appropriate), the shape being determined through self-consistent minimization of the total wave function energy. The localized $\pi_i$ have more qualitative meaning, but it is computationally easier to obtain the equivalent natural orbitals $\pi_g$ and $\pi_u$ and their associated coefficients $\lambda_{g,u}$ through a self-consistent procedure[14] and then convert to the localized picture. At the reactant and product geometries, wave functions were obtained in which an electron-pair expansion was used to represent four of the valence electron pairs (the remaining electron pairs were treated as individual self-consistent doubly occupied orbitals). Thus for the metallacycle state, this expansion was used for both the C–C and Ti–C $\sigma$ bonds, while for the alkylidene–olefin complex, both the C–C and Ti–C $\sigma$ and $\pi$ bonds were treated in this way. Near the reaction saddle point, however, a more general form of self-consistent wave function was required that allowed optimization of spin couplings as well.[34] This was necessary to describe the superposition in eq 7. This more general treatment was accorded only those orbitals that change character during the reaction (i.e., those appearing in eq 5 and 11). Figures 4B,D, 5B, and 6B were obtained by using this approach.

Thermodynamic estimates were obtained by using the GVB orbitals as a basis for configuration interaction (CI) calculations. The dominant configuration placed two electrons in each of the first (or bonding) natural orbitals (e.g., $\pi_u$ above). All excitations were allowed from this configuration within the eight natural orbitals representing the GVB pairs with a quadruple excitation maximum overall (denoted GVB–CI quadruples). These calculations, since they incorporate correlation effects and other excited-state contributions directly, provide accurate total energies for use in computing enthalpy changes.

**C. Geometry Optimization.** The reactant, product, and transition-state geometries were optimized by calculating analytic first derivatives (with respect to coordinate variation) for the total Hartree–Fock energy, using the method of Dupuis and King.[35] Second derivatives were estimated by constructing an approximate force constant matrix from molecular vibrational data and correcting it after each new test geometry via finite difference of analytic first derivatives, essentially as outlined by Schlegel.[36] Test geometries were chosen by stepping in the 30-dimensional coordinate space along a vector obtained by subjecting the most recent first and second derivatives to a damped Newton–Raphson procedure analogous to that proposed by Cerjan and Miller.[37] The "wave function–first derivative–second derivative–step" iterative sequence was repeated for reactant and product states until the wave functions showed an average gradient below 0.001 hartree/bohr and all second derivatives were positive. The second derivatives were used to obtain zero-point frequency and entropy estimates. For the transition state, this sequence was repeated, with steps being directed through the damping procedure away from any minima associated with the smallest second derivative. The smallest (nontranslational, or rotational) second derivative estimates were always close to zero even quite far from the transition state, which hampered the efficiency of the search. The search was initiated by stepping uphill in energy from points near both the reactant and product minima. With some difficulty, the transition-state geometry was optimized to an average gradient of 0.000 51 hartree/bohr.

The validity of geometries based on derivatives of the uncorrelated Hartree–Fock wave function was of some concern. As is well-known, HF calculations frequently predict bond distances that are slightly too short, while GVB calculations err toward slightly long distances. As mentioned above, correlated GVB wave functions were also obtained at test geometries for each of the complexes. While analytic gradients (and thus a thoroughly optimized geometry) could not be obtained by using these wave functions for a detailed comparison, we note that trends in total energies obtained from GVB (and CI) calculations parallelled the HF results for the $\pi$ complex. For the transition-state complex, spin-optimized GVB calculations suggested that a gradient procedure based on correlated wave functions would likely have lead to a slightly different prediction of the transition-state geometry. The geometry shown in Figure 5C comes closest of those tested to representing a saddle point (average HF gradient = 0.006 hartree/bohr) if correlated wave function total energies are used. Using this as the transition-state position leads to a calculated barrier of 6 kcal/mol, about 6 kcal/mol higher than the more rigorously obtained HF-based value. This value, since it was obtained for a geometry that is only approximately optimal, may be taken as an upper bound to the barrier height. GVB calculations carried out for the metallacycle, on the other hand, produced total energy trends during geometry optimization that did not clearly mimic the HF results. In particular, the Ti–C bonds were found to be only 1.96 Å after HF optimization, with a C–Ti–C angle of 83°. Additionally, GVB and GVB–CI calculations were carried out in which ring skeleton angles and bond distances were varied. It was found that Ti–C bond distances increased substantially to 2.12 Å, with a corresponding reduction

(33) Hay, P. J.; Wadt, W. R.; Kahn, L. R. *J. Chem. Phys.* **1978**, *68*, 3059–3066.

(34) A computational procedure developed by F. W. Bobrowicz, based upon: Ladner, R. C.; Goddard, W. A., III *J. Chem. Phys.* **1969**, *51*, 1073–1087. Bobrowicz, F. W. Ph.D. Thesis, California Institute of Technology, Pasadena, 1974.

(35) Dupuis, M.; King, H. F. *J. Chem. Phys.* **1978**, *68*, 3998–4004. Dupuis, M.; Rys, J.; King, H. F. *QCPE* **1981**, *13*, 403.

(36) Schlegel, H. B. *J. Comput Chem.* **1982**, *3*, 214–218.

(37) Cerjan, C. J.; Miller, W. H. *J. Chem. Phys.* **1981**, *75*, 2800–2806.

in C-Ti-C angle to 75.8°. Minimal changes occurred in the remaining angles and distances. The total energy for the complex was reduced by only 4.2 kcal/mol as a result of this further optimization.[38] This final geometry is shown in Figure 1A.

**D. Form of the Transition-State Wave Function.** The wave function superposition represented in eq 7 appears in terms of Young tableau[39] as

$$\psi(TS)_+ = \boxed{\begin{array}{cc}\pi_2 & \pi_3\\ \pi_1 & \pi_4\end{array}} + \boxed{\begin{array}{cc}\pi_1 & \pi_2\\ \pi_3 & \pi_4\end{array}} = \boxed{\begin{array}{cc}\pi_1 & \pi_2\\ \pi_3 & \pi_4\end{array}} \quad \text{(A2)}$$

Because orbital pairs $\pi_1$-$\pi_3$ and $\pi_2$-$\pi_4$ are triplet coupled here, they may be taken as orthogonal without restriction (the antisymmetrizer projects away any nonorthogonalities). The total wave function has an overall singlet spin coupling, and a more complete representation of the transition state must include the remaining linearly independent singlet coupling of these orthogonal orbitals[11g]

$$\psi(TS) = \lambda_1\boxed{\begin{array}{cc}\pi_1 & \pi_2\\ \pi_3 & \pi_4\end{array}} + \lambda_2\boxed{\begin{array}{cc}\pi_1 & \pi_3\\ \pi_2 & \pi_4\end{array}} = \lambda_1\phi_+^T + \lambda_2\phi_+^S \quad \text{(A3)}$$

The second term, $\phi_+^S$, couples the orthogonal orbitals into two open-shell singlet pairs. When the orbitals interact initially, they achieve orthogonality by forming bonding-antibonding pairs, and this term serves to introduce ionic contributions. For localized orbitals that are already orthogonal, such as $d\pi_4$ and $\pi_2$ in section IIIB, $\phi_+^S$ need not be of an ionic form. In precise terms, eq 9 of the text is obtained for $\lambda_1 = \lambda_2$, that is

$$\Psi_+ = \phi_+^T + \phi_+^S \quad \text{(A4)}$$

Thus, as $\phi_+^S$ contributes, the total transition-state wave function becomes better represented by eq 9, or

$$\psi_+ = \boxed{\begin{array}{c}(\pi_1 - \pi_3)(\pi_2 - \pi_4)\\ (\pi_1 + \pi_3)(\pi_2 + \pi_4)\end{array}} \quad \text{(A5)}$$

in terms of tableau.

(38) Total energies from configuration interaction calculations are as follows: metallacycle, -1884.0677; $\pi$ complex, -1884.0534; transition state, -1884.0498; alkylidene + olefin, -1884.0344.

(39) See, for example: Pauncz, R. "Spin Eigenfunctions, Construction and Use"; Plenum Press: New York, 1979.

**Registry No.** $Cl_2TiC_3H_6$, 79953-32-5; $Cl_2TiCH_2(C_2H_4)$, 91158-49-5; $Cp_2TiC_3H_6$, 80122-08-3; $Cp_2TiCH_2(C_2H_4)$, 79105-33-2.

# A Mechanistic Study of the Photochemically Initiated Oxidative Addition of Isopropyl Iodide to Dimethyl(1,10-phenanthroline)platinum(II)

**Ross H. Hill and Richard J. Puddephatt***

*Contribution from the Department of Chemistry, University of Western Ontario, London, Ontario, Canada N6A 5B7.* *Received June 15, 1984*

**Abstract:** The photochemically initiated oxidative addition of isopropyl iodide to dimethyl(1,10-phenanthroline)platinum(II) (**1**) has been studied. Irradiation into the lowest energy MLCT band of **1** ($\lambda$ = 473 nm) leads to iodine atom abstraction from *i*-PrI by the MLCT excited state of **1**. This state is shown to have triplet character since the initiation can be effected with use of a triplet sensitizer (benzophenone) and retarded with use of a triplet quencher (pyrene). The initiation is followed by a free radical chain mechanism of oxidative addition, with isopropyl radicals (which may be trapped with use of the radical trap DMPO) as chain carriers. The reaction is retarded in the presence of radical scavengers. The termination step is shown to involve attack of isopropyl radicals at the methyl or 1,10-phenanthroline ligands of **1** and not the expected combination/disproportionation reaction involving two isopropyl radicals. A kinetic analysis of the reaction in the presence and absence of sensitizer, quencher, or scavenger has led to the determination of several of the key rate constants needed to describe quantitatively the chain reaction.

The framework for discussion of mechanisms of oxidative addition of alkyl halides to transition-metal complexes was established over 10 years ago.[1] Three mechanisms, the $S_N2$ mechanism, with the electron-rich metal center acting as nucleophile, and the free radical chain and nonchain mechanisms have been supported[1,2] (eq 1-3).

$$L_nM + RX \rightarrow [L_nMR]^+X^- \rightarrow L_nMXR \quad (1)$$

$$L_nM + R\cdot \rightarrow [L_nMR]\cdot \xrightarrow{RX} L_nMXR + R\cdot \quad (2)$$

$$L_nM + RX \rightarrow [L_nM]^+\cdot[RX]^-\cdot \rightarrow [L_nMX]\cdot R\cdot \rightarrow L_nMXR \quad (3)$$

A number of techniques have been developed for distinguishing between these mechanisms,[2] but very little is known about the factors which influence whether a reaction will proceed by the free radical chain or nonchain mechanisms or by both mechanisms.[2] This is partly a result of the lack of experimental methods for determining rates of the initiation, propagation, and termination steps of the free radical chain processes. Indeed, even the natures of the initiation and termination steps are obscure in many cases.

The oxidative addition of isopropyl iodide to dimethyl(1,10-phenanthroline)platinum(II) (**1**) occurs slowly under thermal activation according to eq 4, (N-N = phen).[3]

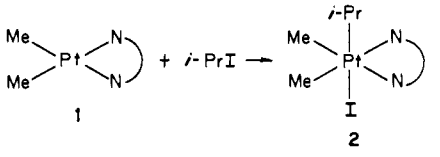


1 2 (4)

(1) (a) Halpern, J. *Acc. Chem. Res.* **1970**, *3*, 386. (b) Bradley, J. S.; Connor, D. E.; Dolphin, D.; Labinger, J. A.; Osborn, J. A. *J. Am. Chem. Soc.* **1972**, *94*, 4043. (c) Lappert, M. F.; Lednor, P. W. *J. Chem. Soc., Chem. Commun.* **1973**, 948.

(2) (a) Lappert, M. F.; Lednor, P. W. *Adv. Organomet. Chem.* **1976**, *14*, 345. (b) Kochi, J. K. "Organometallic Mechanisms and Catalysis"; Academic: New York, 1978; pp 156-168. (c) Labinger, J. A.; Osborn, J. A.; Coville, N. J. *Inorg. Chem.* **1980**, *19*, 3236. (d) Hall, T. L.; Lappert, M. F.; Lednor, P. W. *J. Chem. Soc., Dalton Trans.* **1980**, 1448.

(3) Ferguson, A.; Parvez, M.; Monaghan, P. K.; Puddephatt, R. J. *J. Chem. Soc., Chem. Commun.* **1983**, 267.

0002-7863/85/1507-1218$01.50/0 